UCRL-JC-130102
PREPRINT

Capsule Design for the National Ignition Facility

T. R. Dittrich, S. W. Haan, M. M. Marinak,
D. E. Hinkel, S. M. Pollaine, R. L. McEachern,
R. C. Cook, C. C. Roberts, D. C. Wilson,
P. A. Bradley, and W. S. Varnum

This paper was prepared for submittal to the
25th European Conference on Laser Interaction with Matter
Formia, Italy
May 4-8, 1998

August 1, 1998

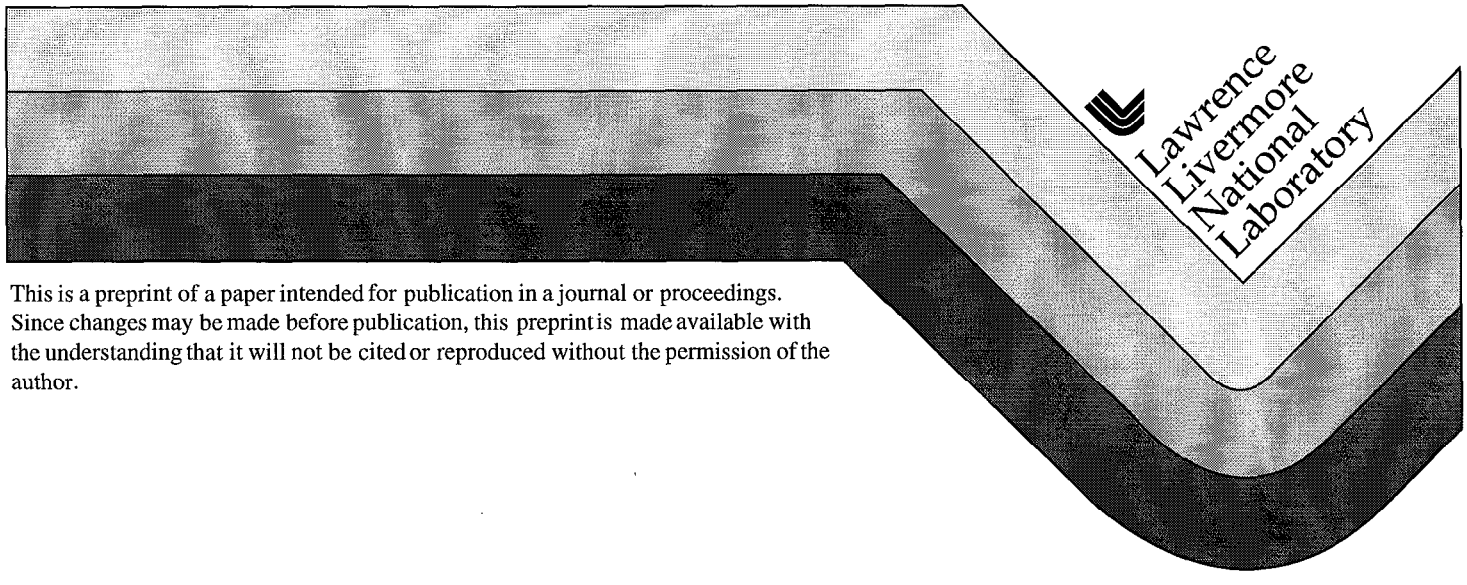

Capsule Design for the National Ignition Facility*

T. R. Dittrich, S. W. Haan, M. M. Marinak, D. E. Hinkel, S. M. Pollaine, R. McEachern, R. C. Cook, C. C. Roberts, *Lawrence Livermore National Laboratory*,
D. C. Wilson, P. A. Bradley, W. S. Varnum, *Los Alamos National Laboratory*.

Abstract. Several choices exist in the design and production of capsules intended to ignite and propagate fusion burn of the DT fuel when imploded by indirect drive at the National Ignition Facility. These choices include ablator material, ablator dopant concentration and distribution, capsule dimensions, and x-ray drive profile (shock timings and strengths). The choice of ablator material must also include fabrication and material characteristics, such as attainable surface finishes, permeability, strength, transparency to radio frequency and infrared radiation, thermal conductivity, and material homogeneity. Understanding the advantages and/or limitations of these choices is an ongoing effort for LLNL and LANL designers. At this time, simulations in one- two- and three- dimensions show that capsules with either a copper doped beryllium or a polyimide ($C_{22}H_{10}N_2O_4$) ablator material have both the least sensitivity to initial surface roughnesses and favorable fabrication qualities. Simulations also indicate the existence of capsule designs based on these ablator materials which ignite and burn when imploded by less than nominal laser performance (900 kJ energy, 250 TW power, producing 250 eV peak radiation temperature). We will describe and compare these reduced scale capsules, in addition to several designs which use the expected 300 eV peak x-ray drive obtained from the nominal NIF laser (1.3 MJ, 500 TW).

Introduction. National Ignition Facility (NIF) (Paisner et al. 1994) capsule designs cover a range of x-ray drive temperatures, ablator materials, and total laser energies. Ablator materials studied to date include polystyrene (CH) doped with bromine (Br) or germanium (Ge), beryllium (Be) doped with copper (Cu), and polyimide ($C_{22}H_{10}N_2O_4$). Numerical simulations show that a capsule design using a CH ablator (Haan *et al.* 1995 & Lindl 1995) requires a dopant material such as Br or Ge to achieve optimum performance when imploded by a 300 eV peak temperature x-ray source obtained from a 1.3 MJ total energy laser. According to simulations, capsule designs using a Be ablator also require doping (e.g., with Cu) in order to achieve optimum performance. Currently, these Be ablator capsule designs span several peak x-ray drive temperatures and total laser energies: 330 eV/1.3 MJ (Krauser *et al.* 1996), 300 eV/1.3 MJ (Dittrich *et al.* 1996), 250 eV/900 kJ (Dittrich *et al.* 1998), 280 eV/1.4 MJ (Bradley *et al.* 1996), and 350 eV/700 kJ (Hinkel *et al.* ____). Capsules using a polyimide ablator do not require any doping and been designed to work at 250 eV/900 kJ and 300 eV/1.3 MJ (Dittrich *et al.* 1996). A novel double shell capsule using a Be+Cu ablator has been designed to work at 320 eV without cryogenic DT fuel (Harris *et al.* 1996). This paper will describe the design and performance of the Be+graded Cu capsule at 250 eV and 900 kJ, and compare the performance of the CH+Br, Be+uniform Cu, and the polyimide capsules, all at 300 eV, 1.3 MJ.

The indirect drive approach to ignition on NIF consists of converting laser light to x-rays in a gold hohlraum. This hohlraum is a cylinder of length 1.0 cm and radius 0.276 cm. To produce the 300 eV peak x-ray drive from a 1.3 MJ total energy laser profile, the laser entrance holes are 50% of the end caps of this cylindrical hohlraum, and the laser beams enter at 23.5, 30.0, 44.5, and 50.0 degrees. A typical 300 eV peak x-ray drive profile from this indirect drive arrangement is shown in Fig. 1.

Each one of the "steps" in the drive profile shown in Fig. 1 launches a shock during the ablation of the capsule. Implosion of a typical NIF capsule will be accomplished by a series

of four shocks. The relative behavior of these shocks can be easily seen in Fig. 2, which is the result of postprocessing an implosion simulation by means of YORICK (Munro, 1995). Shading in this plot is proportional to the logarithmic derivative of the pressure. The vertical axis measures the capsule mass as integrated from the center outward. The horizontal axis measures time as the implosion proceeds. The horizontal white line at a mass value of ~10^{-6} g represents the interface between the DT gas and the DT ice. The horizontal white line at the mass value of 2.0^{-4} g represents the interface between the DT ice and the ablator material. These two interface marker lines remain constant in time since the capsule regional mass does not change. As noted in the plot, the darker shading features represent the inward progress of each of the four shocks. A well tuned implosion consists of having these shocks remain distinct within the DT ice and join only after breaking into the DT gas.

NIF capsules rely on the establishment of a central hotspot in order to ignite. This hotspot contains a small amount of the total fuel mass at high temperature and low density. The hotspot is confined by the remaining fuel at low temperature and high density. After ignition, burn propagates from the hotspot into the remaining fuel. (For a further description of this ignition process, see Lindl 1995 or Dittrich 1998.)

Capsule design at 250eV, 0.9MJ laser energy. Using numerical simulations, we have designed a NIF ignition capsule to operate at both low peak x-ray drive temperature (250 eV) and low total laser energy (900 kJ), simultaneously (a more detailed description can be found in Dittrich *et al.* 1998). These drive conditions are significantly lower than NIF nominal (300 eV and 1.8 MJ) and produce the lowest acceptable implosion velocity and fuel confinement time consistent with achieving ignition. This capsule design, shown schematically in Fig. 3, uses cryogenic DT fuel which is assumed to be deposited on the inside of the ablator shell by the technique of beta-layering (Hoffer 1988). The Be ablator has a radially varying concentration of Cu to shield the fuel from radiation preheat and to minimize hydrodynamic instability at the DT-Be interface. Cu is distributed in the following manner, starting from the inside of the Be shell: 4.0μm, 0.0%Cu; 4.0μm, 0.55%Cu; 38μm, 1.10%Cu; 11μm, 0.55%Cu; 63μm, 0.0%Cu. All concentrations are atomic fractions. One-dimensional implosion simulation of this capsule gives the following performance: yield, 6.8MJ; mass-weighted implosion velocity of the fuel, 0.034cm/ns; absorbed energy, 114kJ; $\rho\Delta r_{fuel}$, 1.28g/cm^2.

Capsule fusion yield is a function of the initial ablator thickness. To find the optimum thickness for this Be+graded Cu ablator capsule, we compare the 1-D simulated performance of several designs, each with a unique ablator thickness. The results of this comparison are shown in Fig. 4. For each of these implosions, optimum shock timing is maintained by making small timing adjustments to the x-ray drive profile. Each capsule absorbs the same total amount of x-ray energy by adjusting its initial overall size. Lastly, the DT mass is held constant for each design. Based on this scan of thicknesses, a capsule with an ablator thickness of 121.5 μm gives peak yield. For thinner ablator capsules, the ablator burns thru leading to poor fuel entropy and low $\rho\Delta r_{hotspot}$. For thicker ablator capsules, the fuel acquires a lower imploding kinetic energy which leads to a lower ion temperature in the ignition hotspot. Curves similar to that shown in Fig. 4 can be generated for capsules with other levels of Cu dopant. Maintaining the design constraints described above, 1-D performance is optimum (6.8 MJ) for the total amount of Cu dopant (0.082mg) as shown in Fig. 4. Increasing the total amount of Cu dopant to 0.132 mg causes the peak yield to decrease to 4.4 MJ for an ablator thickness of 115 μm. Decreasing the total amount of Cu dopant to 0.010 mg causes the peak yield to decrease to 4.2 MJ for an ablator thickness of 142 μm.

To study the sensitivity of this capsule to Rayleigh-Taylor and/or Richtmeyer-Meshkov instability, we must have estimates of the wavelengths and amplitudes of perturbations likely to exist on both the gas-ice interface and the ablator outer surface. Laboratory charactertization of the achievable DT gas-ice surface roughness shows that perturbations at this interface may be described by a mode spectrum having a total rms of 1.0 μm (Hoffer *et al.* 1996). Fabrication of Be-Cu shells as described here is currently under development, therefore, their surface roughness mode spectrum is assumed to be similar to that obtained on Nova plastic capsules. The best suface obtained on a Nova plastic shell to date has a total rms of 10 nm. These two surface characterizations provide estimates of the contributions from each individual perturbation mode or wavelength.

Figure 5 shows how capsule yield varies as a function of initial DT ice surface rms, according to LASNEX 2-D implosion simulations. The surface perturbation configured in these simulations includes modes 12 to 160, combined with randomly chosen phases. As illustrated in Fig. 5, this capsule is very sensitive to roughness on the DT ice surface. At 1.0 μm rms initial roughness, capsule yield is less than 1MJ. Each of these 2D simulations has no surface roughness configured on the ablator surface. The 1.0 μm rms ice surface roughness quoted above may be improved to about 0.7 μm rms by means of radio frequency heating of the DT. However, the metallic nature of this Be-Cu shell precludes using this technique.

Figure 6 shows how capsule yield varies as the ablator outer surface initial roughness is varied, according to numerical simulation. As with the ice surface, the multimode ablator surface perturbation is a combination of modes 12 to 160. These yield results are from simulations which include 0.47 μm rms roughness on the DT ice surface. With 10 nm rms ablator roughness (and 0.47 μm DT ice surface roughness) the BeCu capsule described above is estimated to produce 3.5MJ, or about 50% of clean 1D yield. Achieving 10-20 nm rms surfaces on Cu doped Be is currently being investigated. At the low drive conditions described above, this Be+graded Cu ablator capsule is marginally viable.

Future work at the below-nominal drive conditions of 250 eV peak radiation temperature and 900 kJ total laser energy will investigate ways to reduce this Be+graded Cu capsule's sensitivity to DT ice surface roughness. Also, we are currently investigating the feasibility of low drive capsules using polyimide ablators. A design exists which produces 4.0 MJ in 1-D simulation, has a mass weighted implosion velocity of 0.036 cm/ns, absorbs 114 kJ and has a $\rho\Delta r_{fuel}$ of 1.26 g/cm^2. At this time, there exists no 2-D implosion stability analysis for this design.

Capsule designs at 300eV, 1.3MJ laser energy. Several capsules have been designed to operate at the nominal x-ray drive peak temperature of 300 eV, obtained from a 1.3 MJ total energy laser. We choose three of these capsules for comparison. These three capsules have different ablator materials, CH+Br+O, Be+Cu and polyimide, but have similar DT fuel implosion characteristics. One-dimensional performance characteristics of these three capsules are shown in Table 1. Implosion and burn of each of these has been simulated using the 3-D code HYDRA to estimate the sensitivity to multimode perturbations on the DT ice surface and the ablator outer surface (more detail can be found in Marinak *et al.* 1998). These 3-D simulations studied modes 15-120 configured on a 15 degree portion of each capsule. This study shows that modes from ~60 to ~100 dominate perturbation growth before peak implosion velocity, and modes from ~15 to ~20 dominate growth after implosion velocity. According to HYDRA, capsules will ignite if spikes penetrate up to one third of the way into the hotspot.

Three-dimensional simulations show that for a given ablator roughness, the Be+Cu capsule can tolerate the roughest DT ice layers. Figure 7 shows how capsule yield varies as the DT

ice surface roughness is varied. Each of these simulations includes 10 nm rms ablator roughness. The Be+Cu and the polyimide capsule show little yield reduction for ice roughness at the native value of 1.0 μm rms. Figure 8 shows how capsule yield varies as the ablator surface roughness is varied. Each Be+Cu simulation includes a DT ice surface roughness of 1.0 μm rms. Since the smoothness of the DT ice surface in either the CH+Br or the polyimide capsule can be enhanced by means of radio frequency heating, each of these simulations assumes a 0.5 μm rms ice roughness. Both the Be+Cu and the polyimide capsule show similar sensitivity to ablator surface roughness. However, the CH+Br capsule can tolerate no more than ~18 nm rms ablator roughness before failure.

Capsule fabrication issues. Each of the ablator materials described above have fabrication advantages and disadvantages. LANL has successfully fabricated a NIF size capsule by the brazing together machined hemispheres of uniformly doped Be (Margevicius *et al.* 1998). These hemispheres were joined in vacuum; techniques for filling this capsule with DT fuel are under development and may require fill holes and fill plugs in the Be shell. Adequate smoothness of the resulting outer surface of this Be capsule can be achieved by lapping. However, since Be is a metal, no active ice surface smoothing is possible. Also, since Be is opaque to visible light, no ice inspection is possible during the layer forming process.

LLNL has fabricated NIF size capsules by sputter depositing the Be on a CH mandrel (McEachern *et al.* 1997); this technique is compatible with including radially varying doping. However, it suffers from the same drawbacks as for the machined hemispheres, such as lack of active ice smoothing, and the inability to inspect ice layer formation. Techniques for filling this capsule with DT fuel are also being developed. Layer thicknesses of 150 μm have been deposited on 3 μm CH mandrels. Sphere mapper traces of these sputter deposited Be capsules show that the surface roughness achieved is within a factor of two of that required for marginal performance. Adding boron to Be during this sputter-deposition process significantly reduces surface roughness. Atomic force microscope images of 5 μm thick films show that Be+9% (atomic) B gives a 19 nm rms surface and Be+13% (atomic) B gives a 2.5 nm rms surface.

As a NIF capsule ablator material, Polyimide ($C_{22}H_{10}N_2O_4$) has several fabrication advantages. The fabrication process consists of monomer deposition (at a rate of 3-4 μm/hr) followed by thermal processing to form high strength polyimide. Deposition on flat substrates shows surface finishes smoother than 10 nm rms. This material is permeable to DT gas, therefore, filling this capsule with fuel appears straightforward. Also, polyimide is transparent to optical frequency light, which will allow visual inspection of DT ice layer formation. Transparency to infrared light and radio frequency radiation will allow active ice surface smoothing after the ice layer has been formed.

Conclusion. NIF capsules have been designed using several different ablator materials, x-ray drive temperatures, and laser energies. Simulations of a Be+graded Cu ablator NIF capsule indicate that 250 eV and 900 kJ are the lowest feasible x-ray drive temperature and laser energy consistent with achieving ignition. Three-dimensional HYDRA simulations predict Be+Cu and polyimide capsules at 300 eV drive have the smallest sensitivity to DT ice roughness and ablator roughness. Material properties and performance complicate the choice for the optimum NIF capsule ablator.

This work was performed under the auspices of the U.S. DOE by LLNL under contract No. W-7405-Eng-48.

Table 1. Performance characteristics of three NIF capsule designs driven at 300 eV peak x-ray radiation from a 1.3 MJ total energy laser.

Ablator Material	CH+Br+O	Be+Cu	Polyimide
Absorbed Energy (kJ)	153	173	154
$\rho\Delta r_{fuel}$ (g/cm^2)	1.65	1.58	1.67
Yield (MJ)	17.6	17.1	18.7
$V_{fuel,\ mass\text{-}wtd}$ (cm/ns)	0.041	0.039	0.038

Figure Captions

Fig. 1. X-ray radiation temperature versus time obtained from absorption of laser light in a cylindrical hohlraum. This profile has a peak temperature of 300 eV, from a total laser energy of 1.3 MJ.

Fig. 2. Result of postprocessing a one-dimensional simulation using YORICK. Shading in this plot is proportional to the logarithmic derivative of the pressure.

Fig. 3. Schematic diagram of a NIF ignition capsule driven by a 250 eV peak temperature x-ray drive obtained from a 0.9 MJ total energy laser.

Fig. 4. Capsule fusion yield as a function of initial ablator thickness for the 250 eV - 0.9 MJ design, according to one-dimensional numerical simulation. Peak yield is obtained at an ablator thickness of 121.5 μm.

Fig. 5. Fusion yield as a function of initial DT ice-gas surface roughness for the 250 eV - 0.9 MJ capsule design. These results are from two-dimensional simulation of multimode perturbations. Initial ablator surface roughness for these simulations is 0.0 μm rms.

Fig. 6. Fusion yield as a function of initial ablator surface roughness for the 250 eV - 0.9 MJ capsule design. These results are from two-dimensional simulation of multimode perturbations. Initial DT gas-ice surface roughness for each simulation is 0.47 μm rms.

Fig. 7. Fusion yield as a function of initial DT gas-ice surface roughness for three capsules driven at 300 eV and 1.3 MJ. These results are from three-dimensional simulation of multimode perturbations, using the HYDRA code. Initial ablator surface roughness for these simulations is 10 nm rms.

Fig. 8. Fusion yield as a function of initial ablator surface roughness for three capsules driven at 300 eV and 1.3 MJ. These results are from three-dimensional simulation of multimode perturbations, using the HYDRA code. Initial gas-ice surface roughness was 1.0 μm rms for the Be+Cu capsule and 0.5 μm rms for the CH+Br+O and the polyimide capsule.

References

Bradley, P. A. and Wilson, D. C. 1996 *Bull. Am. Phys. Soc.* **41** 1557.

Dittrich, T. R., Haan, S. W., Pollaine, S., Burnham, A. K., Strobel, G. L., Fusion Technology **31** (4) 402 (1997).

Dittrich, T. R., W. Haan, S. W., Marinak, M. M., Pollaine, S. M., McEachern, R. 1998 *Phys. Plasmas* (accepted for publication).

Haan, S. W., Pollaine, S. M., Lindl, J. D., Suter, L. J., Berger, R. L., Powers, L. V., Alley, W. E., Amendt, P. A., Futterman, J. A., Levedahl, W. K., Rosen, M. D., Rowley, D. P., Sacks, R. A., Shestakov, A. I., Strobel, G. L., Tabak, M. Weber, S. V., Zimmerman, G. B., Krauser, W. J., Wilson, D. C., Coggeshall, S. V., Harris, D. B., Hoffman, N. M., Wilde, B. H. 1995 *Phys. Plasmas* **2** (6), 2480.

Harris, D. B., Varnum, W. S. 1996 *Bull. Am. Phys. Soc.* **41** 1479.

Hinkel, D. E., (reference???)

Hoffer, J. K. and Foreman, L. R. 1988 *Phys. Rev. Lett.* **60** (13) 1310.

Hoffer, J. K., Foremna, L. R., Sanchez, J. J., Mapoles, E. R., Sheliak, J. D. 1996 *Fusion Technology* **30** (529).

Krauser, W. J., Hoffman, N. M., Wilson, D. C., Wilde, B. H., Varnum, W. S., Harris, D. B., Swenson, F. J., Bradley, P. A., Haan, S. W., Pollaine, S. M., Wan, A. S., Moreno, J. C., Amendt, P. A. 1996 *Phys. Plasmas* **3** (5) 2084.

Margevicius, R., Salzer, L., Salazar, M., Adams, C., Thoma, D., Foreman, L. *1998 presented at Target Fabrication Meeting '98, Jackson Hole, Wyoming.*

McEachern, R., Alford, C., Cook, R. Makowiecki, D., Wallace, R. *1997 Fusion Technology* **31** (4) 435.

Munro, D. H. 1995 *Computers in Physics* **9** (6) 609.

Lindl, J. D. 1995 Phys. Plasmas **2** (11) 3393.

Marinak, M. M., Haan, S. W., Dittrich, T. R., Tipton, R. E., Zimmerman, G. B. 1998 *Phys. Plasmas*, **5** (4) 1125.

Paisner, J. A., Boyes, J. D., Kumpan, S. A., Lowdermilk, W., H., Sorem, M. S. 1994 Laser Focus World **30** (75).

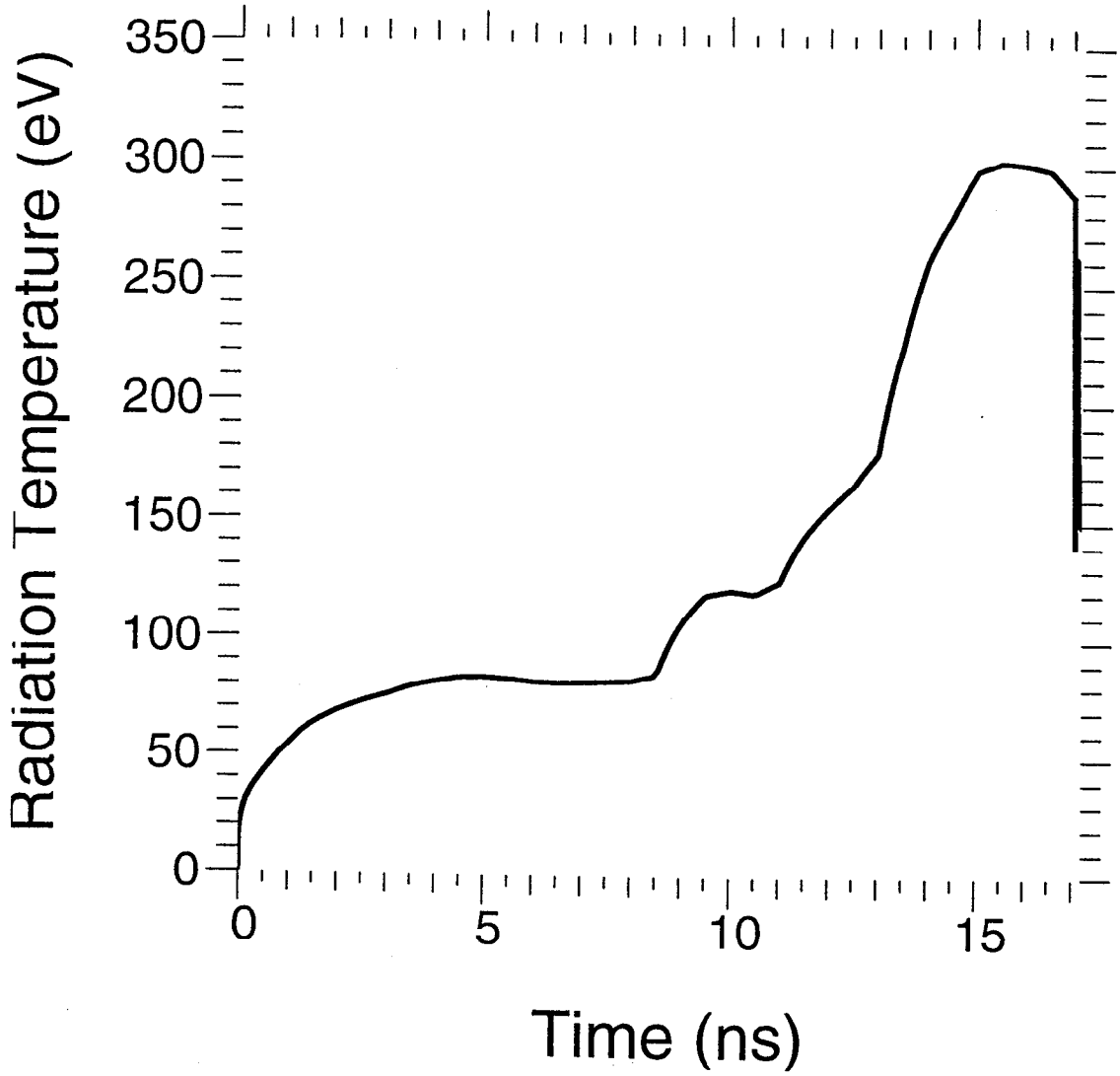
Radiation Temperature (eV)
350
300
250
200
150
100
50
0
0
5
10
15
Time (ns)

FIG. 1

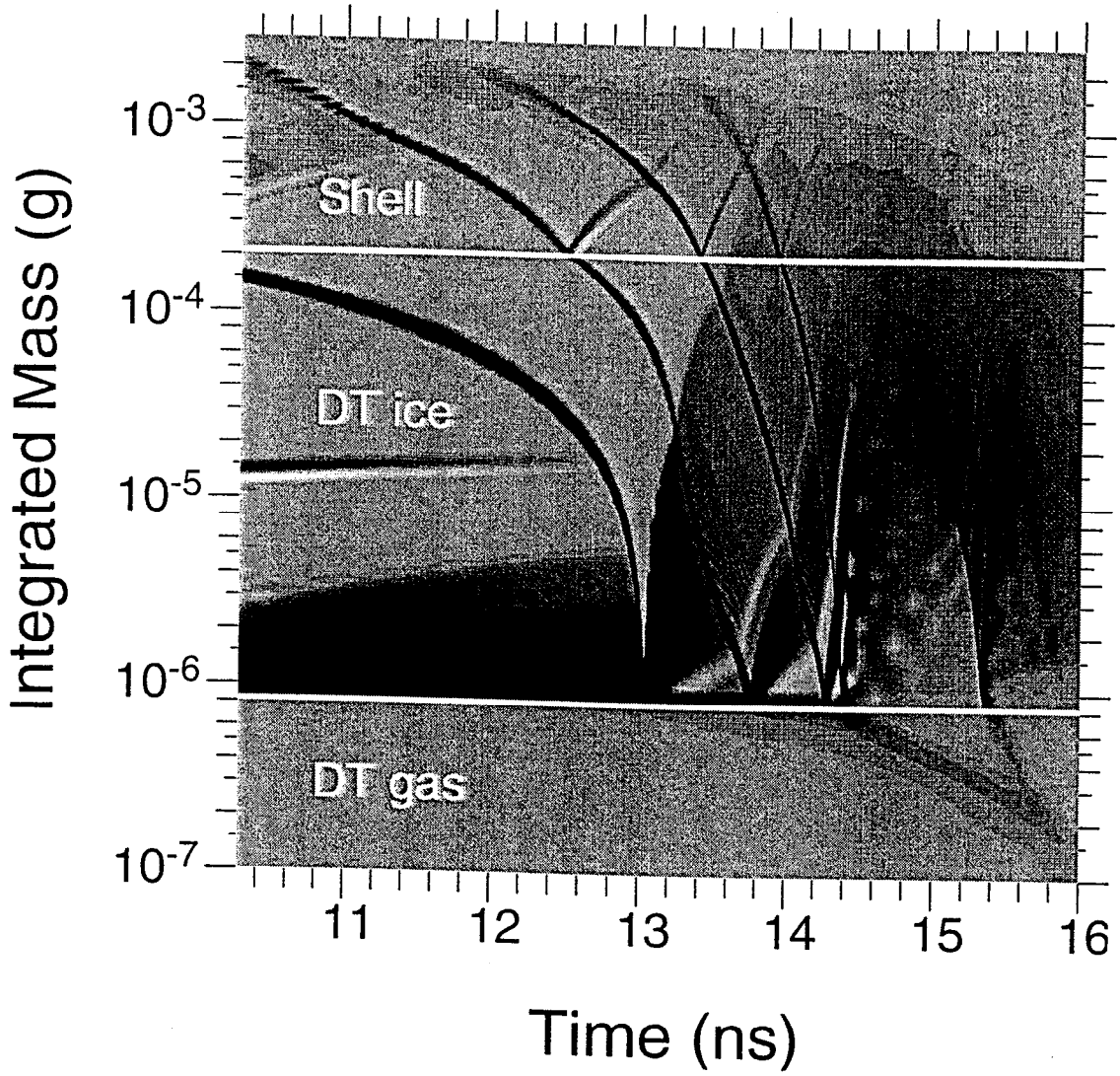
Integrated Mass (g)
10-3
10-4
10-5
10-6
10-7
Shell
DT ice
DT gas
11
12
13
14
15
16
Time (ns)

FIG 2

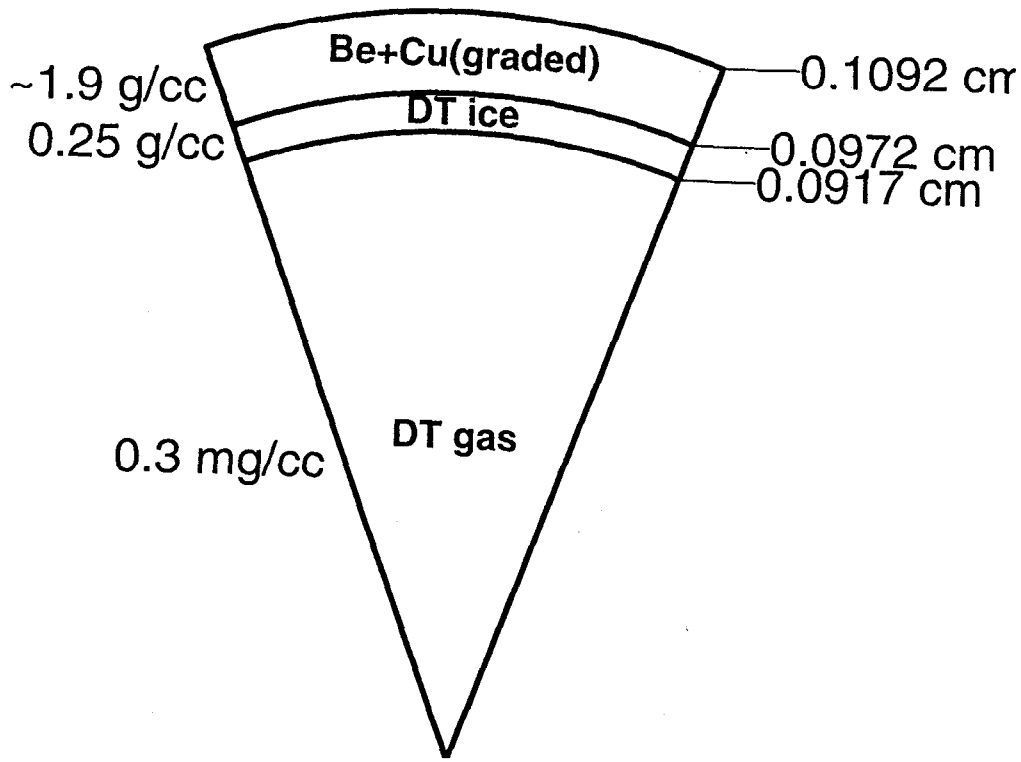
Be+Cu(graded)
~1.9 g/cc
0.25 g/cc
DT ice
0.1092 cm
0.0972 cm
0.0917 cm
DT gas
0.3 mg/cc

FIG 3

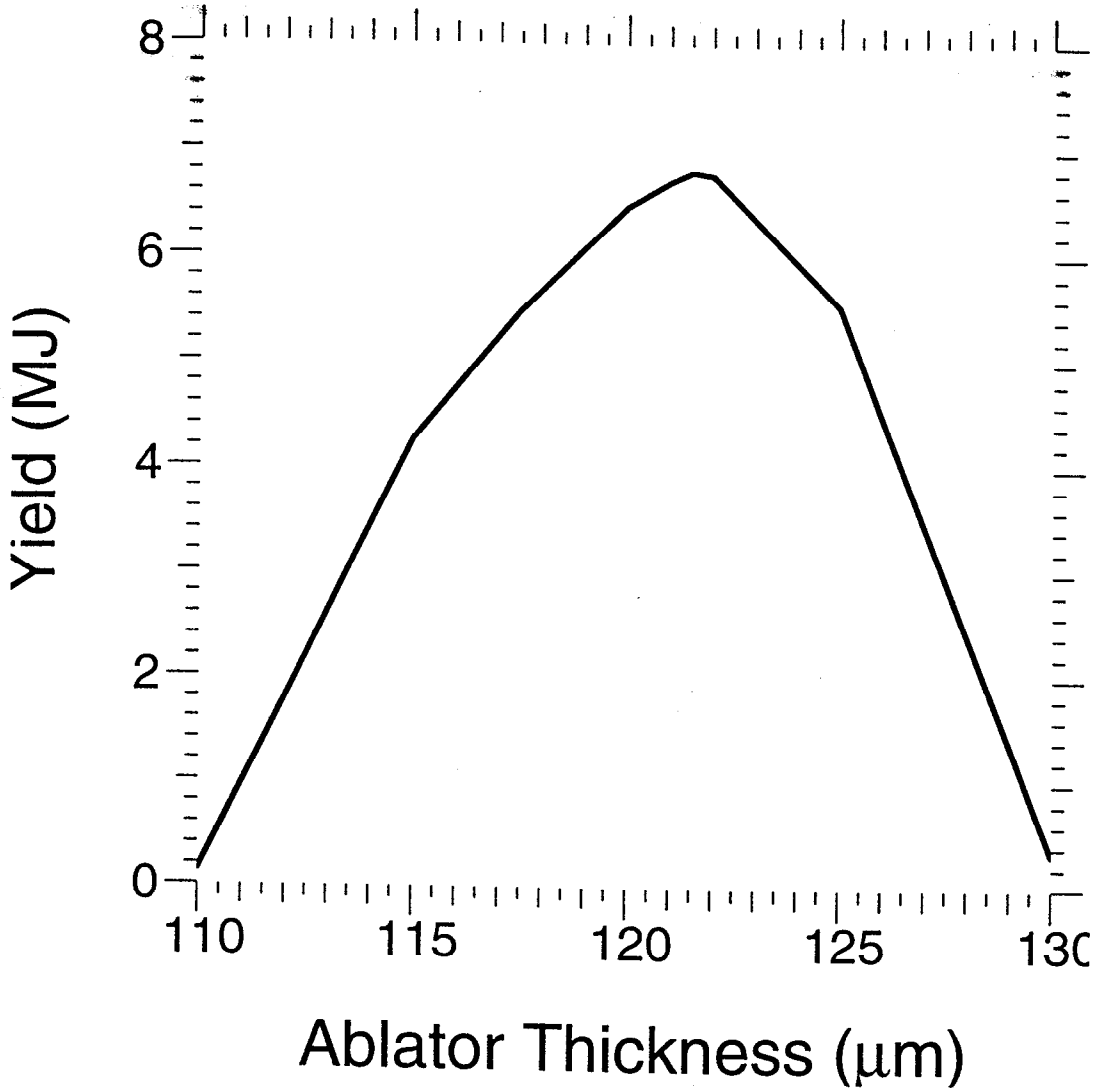

FIG 4

vg971114.i

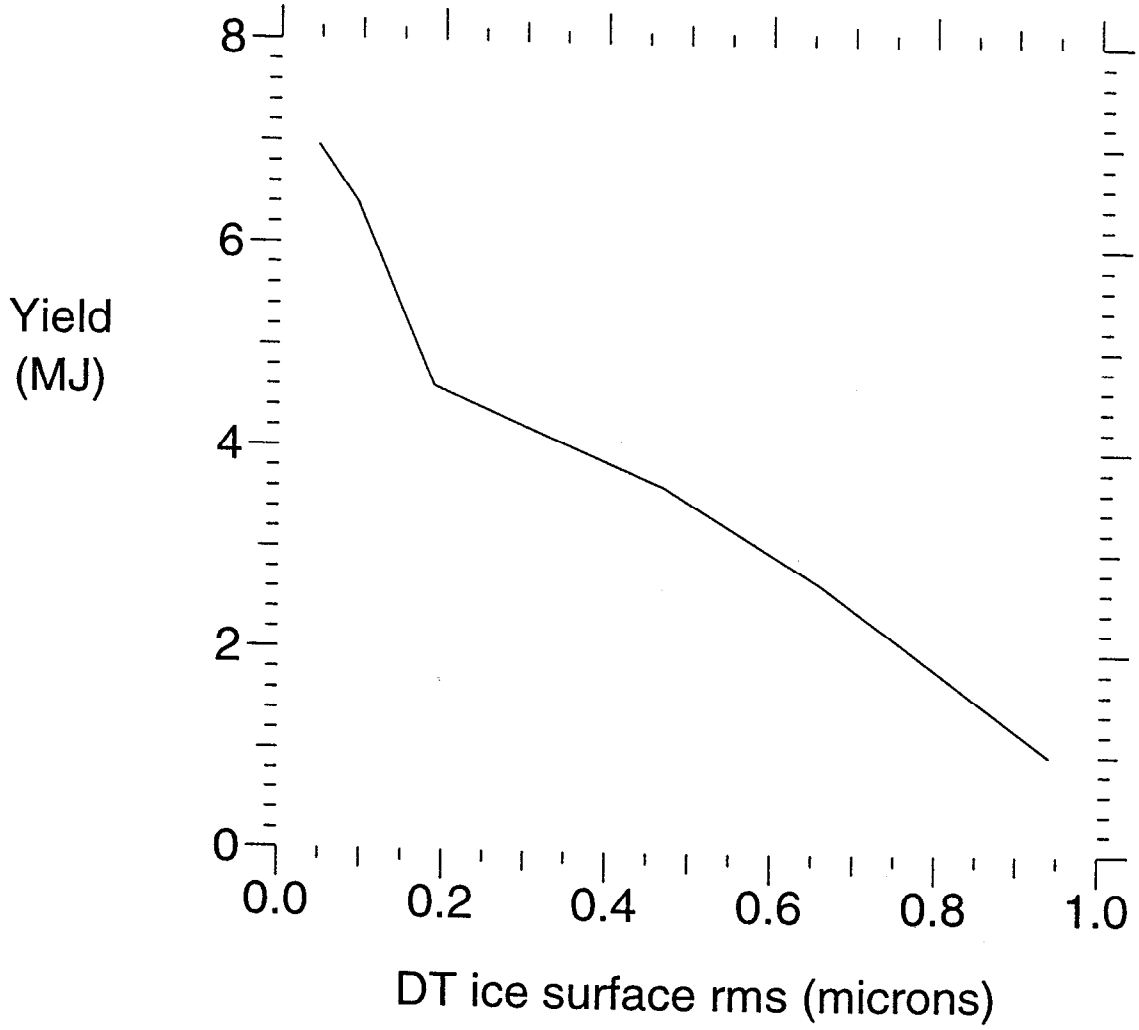

FIG 5

vg971115.i

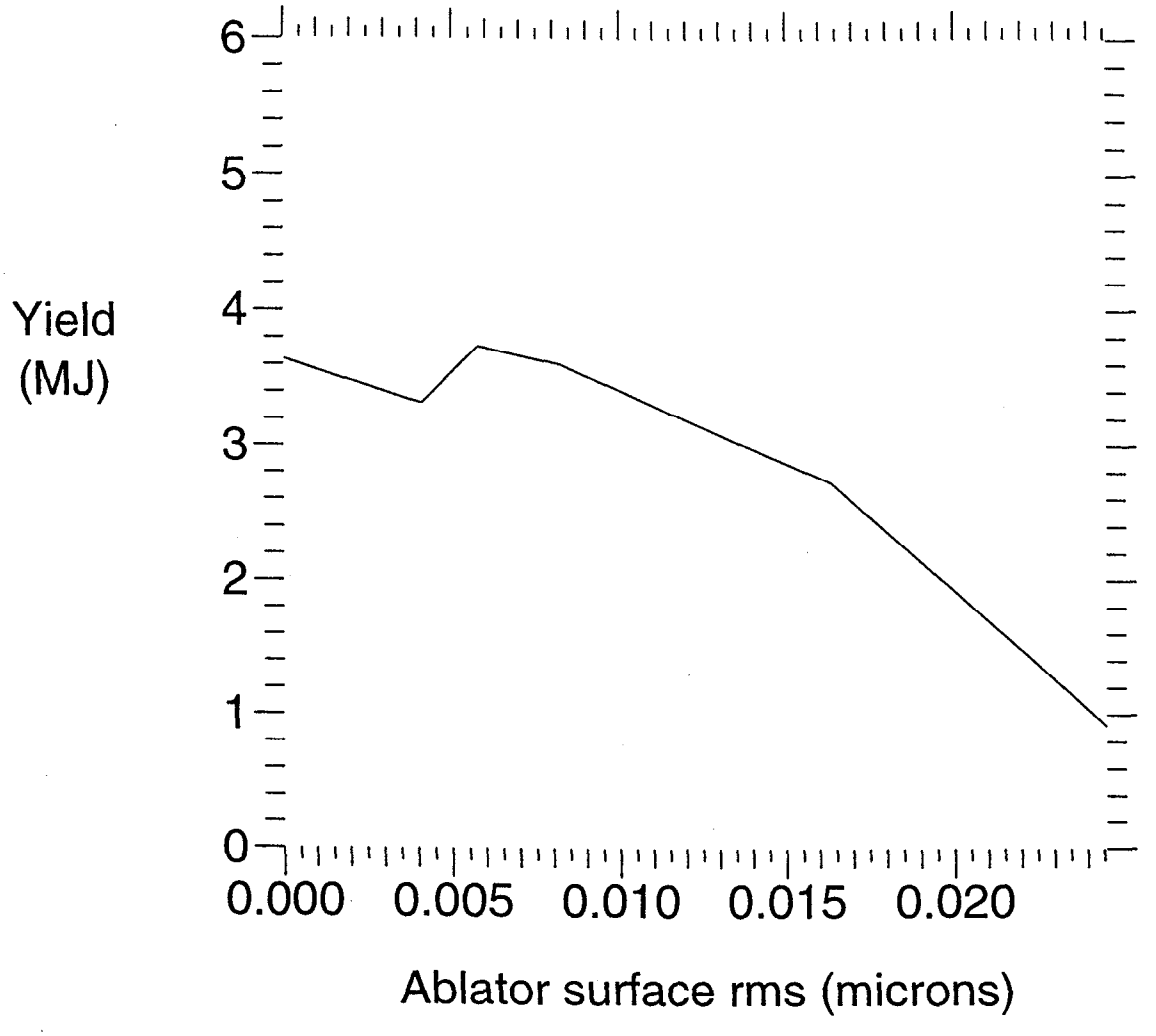

FIG 6

vg980130.i

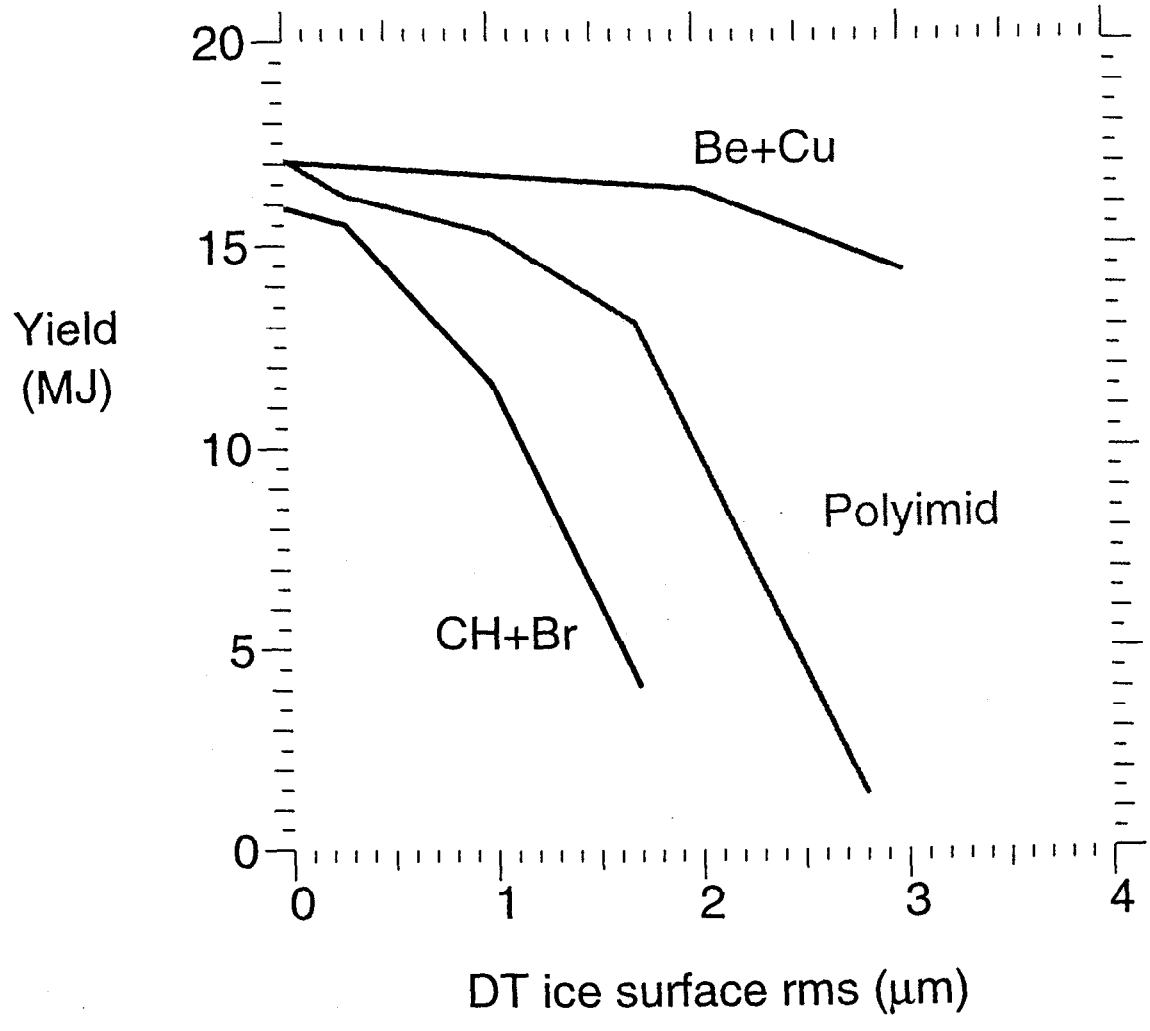

FIG 7

vg980130.i

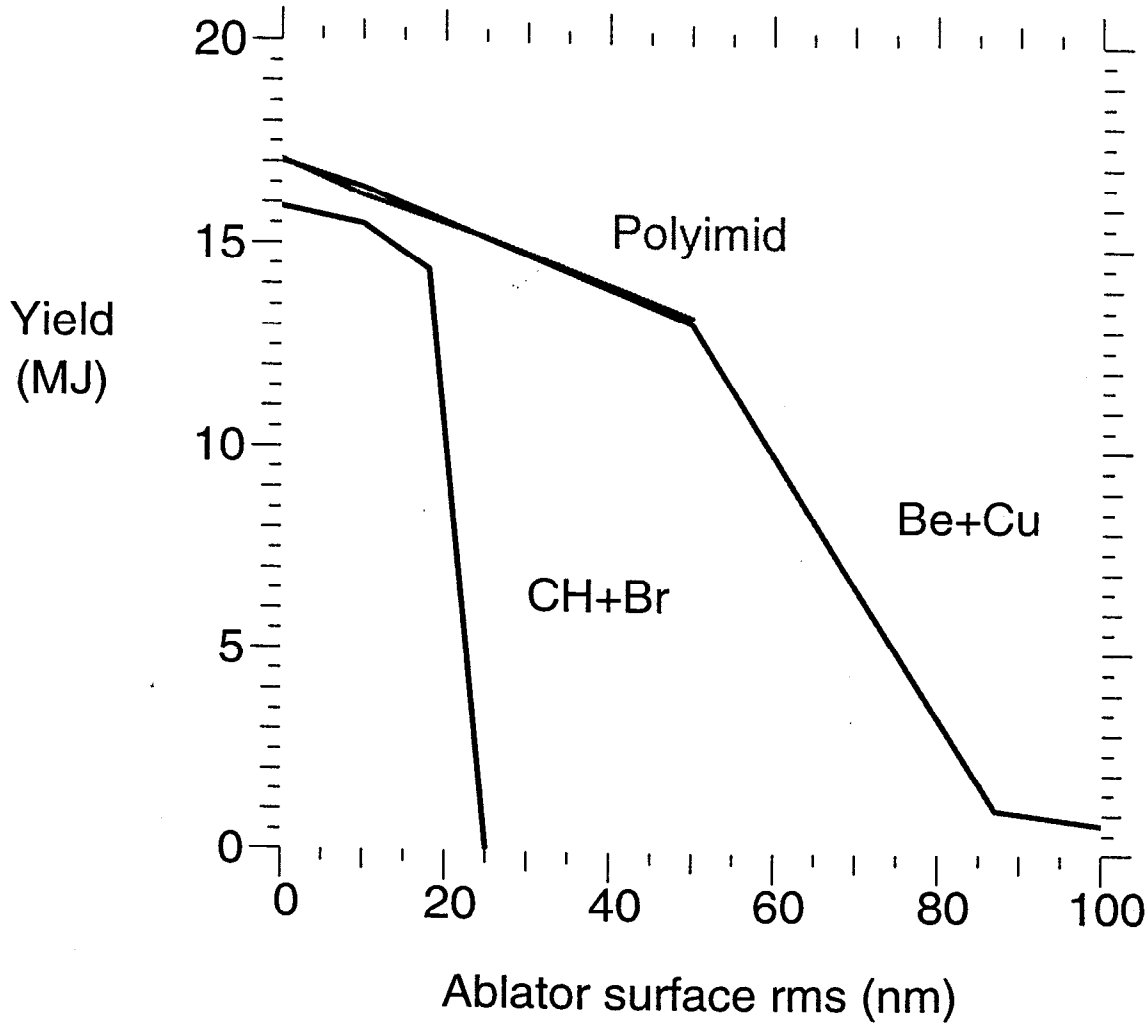

FIG 8